10th World Congress on Structural and Multidisciplinary Optimization
May 19 -24, 2013, Orlando, Florida, USA

Optimal Free-form Design of Shell Structure for Stress Minimization

Masato Yonekura[1], Masatoshi Shimoda[2] and Yang Liu[3]

[1]Graduate School of Toyota Technological Institute, Nagoya, Japan, sd12444@toyota-ti.ac.jp
[2] Toyota Technological Institute, Nagoya, Japan, shimoda@toyota-ti.ac.jp
[3] Toyota Technological Institute, Nagoya, Japan, liuyang@toyota-ti.ac.jp

1. Abstract
This paper presents a parameter-free free-form optimization method for the strength design of shell structure. The maximum von Mises stress is minimized subject to the volume constraint. The optimum design problem is formulated as a distributed-parameter shape optimization problem under the assumptions that a shell is varied in the out-of-plane direction to the surface and the thickness is constant. The issue of non-differentiability inhered in this minmax problem is avoided by transforming the local measure to a smooth differentiable integral functional by using the Kreisselmeier-Steinhauser function The shape gradient function and the optimality conditions derived using the material derivative method are applied to the free-form optimization method for shells. With this method, the smooth optimal free-form of a shell structure is obtained without any shape design parameterization, while minimizing the maximum stress. The validity of this method is verified through two design examples.
2. Keywords: Optimum Design; Shape Optimization; Shell; Free-form; KS Function.

3. Introduction
Shell structures with thinness and lightness are extensively used as the structural components in various industrial products, structures and constructions. In the design of shell structures, it is important to optimize their forms, or curvature distributions to achieve required mechanical performances such as stiffness, natural frequency, maximum stress and buckling load. In our previous works, we proposed a non-parametric free-form optimization method of shell structures, and applied it to stiffness design problems [1][2][3] and vibration design problems[4]. With the method, an optimum shell with smooth free-form surface can be obtained without any shape parameterization which is inevitable process in general parametric shape optimization methods.
Focusing on shape optimization of shell structures, the methods can be categorized into parametric and non-parametric methods in terms of design variables. Although most previously proposed shape optimization methods for shells [5][6] are parametric methods, which require parameterization of the shape in advance and the obtained shape is strongly influenced by the parameterization process, our method is classified as a non-parametric method. The proposed method and its features will be described in the following sections. Another non-parametric method with a filter for smoothing was presented by Bletzinger et al. [7].
In this paper, we newly apply this method to a maximum stress minimization problem as a strength design problem of shell structures. The issue of non-differentiability is inherent to this stress minmax problem because of the singularity of maximum stress, making it theoretically difficult to determine directly the sensitivity function of the local objective functional. This issue is avoided by transforming the local measure to an integral functional by using the Kreisselmeier-Steinhauser (*KS*) function [8] to transform the local objective functional into the smooth differentiable integral functional.
This stress minmax problem is formulated in a function space. The maximum von Mises stress extracted by the *KS* function and a volume are defined as the objective and constraint functional, respectively. It is assumed that the shell is varied in the normal direction to the surface and the thickness is constant. The shape sensitivity function for this problem is theoretically derived using the material derivative method and the adjoint variable method. The shape sensitivity function derived is applied to the shell surface as the traction force to vary the shape under elastically supported condition. Two design examples calculated by this method are demonstrated. The optimum shapes with beads and the iteration histories show the effectiveness of the proposed method as a solution to the stress minmax problem.

4. Governing equation of shell structure
As shown in Fig. 1 and Eqs. (1)-(3), consider a shell having an initial bounded domain $\Omega \subset \mathbb{R}^3$ (boundary of $\partial\Omega$), mid-area A (boundary of ∂A), side surface S and plate thickness h. The notations $(\boldsymbol{x}_1, \boldsymbol{x}_2, \boldsymbol{x}_3)$ and $(\boldsymbol{X}_1, \boldsymbol{X}_2, \boldsymbol{X}_3)$ in Fig. 1 indicate the local coordinate system and the global coordinate system, respectively.

$$\Omega=\left\{ \quad (x_1,x_2,x_3)\in\mathbb{R}^3 \middle| \ (x_1,x_2)\in A\subset\mathbb{R}^2, x_3\in\left(-\frac{h}{2},\frac{h}{2}\right) \right\}, \tag{1}$$

$$\Omega = A\times(-\frac{h}{2},\frac{h}{2}), \qquad S=\partial A\times(-\frac{h}{2},\frac{h}{2}). \tag{2)(3}$$

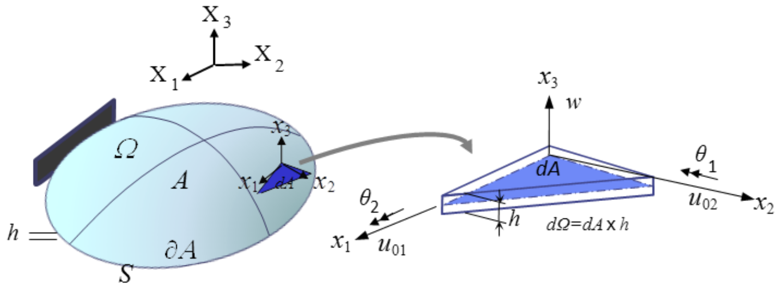

Fig. 1 Coordinate system and DOF of shell

The Mindlin-Reissner plate theory is applied concerning plate bending, and coupling of the membrane stiffness and bending stiffness is ignored. The weak form equation in terms of $(\boldsymbol{u}_0, w, \boldsymbol{\theta})$ can be expressed as Equation (4).

$$a((\boldsymbol{u}_0,w,\boldsymbol{\theta}),(\bar{\boldsymbol{u}}_0,\bar{w},\bar{\boldsymbol{\theta}}))=l((\bar{\boldsymbol{u}}_0,\bar{w},\bar{\boldsymbol{\theta}})), \quad \forall(\bar{\boldsymbol{u}}_0,\bar{w},\bar{\boldsymbol{\theta}})\in U, \quad (\boldsymbol{u}_0,w,\boldsymbol{\theta})\in U, \tag{4}$$

where where $\{u_{0\alpha}\}_{\alpha=1,2}$, w and $\{\theta_\alpha\}_{\alpha=1,2}$ express the in-plane displacement, out-of-plane displacement and rotational angle of the mid-area of the plate, respectively. $\bar{(\ )}$ expresses a variation, and U expresses admissible space in which the given constraint conditions of $(\boldsymbol{u}_0, w, \boldsymbol{\theta})$ is satisfied. In addition, the bilinear form $a(\cdot,\cdot)$ and the linear form $l(\cdot)$ are defined respectively as shown below.

$$a((\boldsymbol{u}_0,w,\boldsymbol{\theta}),(\bar{\boldsymbol{u}}_0,\bar{w},\bar{\boldsymbol{\theta}}))=\int_\Omega\{C_{\alpha\beta\gamma\delta}(u_{0\alpha,\beta}-x_3\theta_{\alpha,\beta})(\bar{u}_{0\gamma,\delta}-x_3\bar{\theta}_{\gamma,\delta})+C^S_{\alpha\beta}\gamma_\alpha\bar{\gamma}_\beta\}d\Omega, \tag{5}$$

$$l((\bar{\boldsymbol{u}}_0,\bar{w},\bar{\boldsymbol{\theta}}))=\int_A(f_\alpha\bar{u}_{0\alpha}-m_\alpha\bar{\theta}_\alpha+q\bar{w})dA+\int_{\partial A}(N_\alpha\bar{u}_{0\alpha}ds-M_\alpha\bar{\theta}_\alpha+Q\bar{w})ds, \tag{6}$$

where $\{C_{\alpha\beta\gamma\delta}\}_{\alpha,\beta,\gamma,\delta=1,2}$ and $\{C^S_{\alpha\beta}\}_{\alpha,\beta=1,2}$ express an elastic tensor including bending and membrane components, and an elastic tensor with respect to the shearing component, respectively. Moreover, $\boldsymbol{f}=\{f_\alpha\}_{\alpha=1,2}$, $\boldsymbol{m}=\{m_\alpha\}_{\alpha=1,2}$, q express an out-of-plane load per unit area, an in-plane load and an out-of-plane moment per unit area, respectively. $\boldsymbol{N}=\{N_\alpha\}_{\alpha=1,2}$, $\boldsymbol{M}=\{M_\alpha\}_{\alpha=1,2}$, Q express an in-plane load, a shearing force and a bending moment per unit length, respectively. The tensor subscript notation uses Einstein's summation convention and a partial differential notation for the spatial coordinates $(\cdot)_{,i}=\partial(\cdot)/\partial x_i$.

5. Optimum strength design problem of shell structure

5.1. Domain variation

Consider that a linear elastic shell structure having an initial domain Ω , mid-area A, boundary ∂A and side surface S undergoes domain variation $\boldsymbol{V}$ (design velocity field) in the out-of-plane direction such that its domain, mid-area, boundary and side surface become Ω_s , A_s , ∂A_s , and S_s , respectively as shown in Fig. 2. It is assumed that the plate thickness h remains constant under the domain variation. The subscript s expresses the iteration history of the domain variation. The free-form optimization method explained later is a method for determining the optimal domain variation $\boldsymbol{V}$ of shell structures.

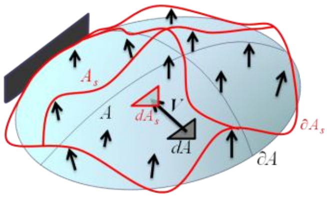

Fig. 2 Domain variation by V

5.2. Stress minmax problem

The non-parametric shape optimization problem with the objective of minimizing the maximum value of von Mises stress on both sides of a shell structure can be formulated as shown below, subject to constrains of volume and the state equation in Eq. (2).

$$\text{Given} \quad A_0, \hat{M}, \tag{7}$$

$$\text{find} \quad \boldsymbol{V} \text{ or } \Omega_s, \tag{8}$$

$$\text{that minimize} \quad \max_{x \in \Omega} \frac{\sigma_M(\boldsymbol{x})}{\sigma_a}, \tag{9}$$

$$\text{subject to} \quad \text{Equation (2) and} \quad M(=\int_A h dA) \leq \hat{M}, \tag{10)(11}$$

where M and $\hat{M}$ denote the volume and its constraint value, respectively. $\sigma_M(\boldsymbol{x})$ is von Mises stress defined as Eq. (12) and σ_a is a constant for the normalization.

$$\sigma_M^2 = \frac{1}{2}\left\{ \left(\sigma_{11} - \sigma_{22}\right)^2 + \sigma_{11}{}^2 + \sigma_{22}{}^2 + 6\left(\sigma_{12}^2 + \sigma_{23}^2 + \sigma_{31}^2\right) \right\}, \tag{12}$$

The issues of non-differentiability are inherent to stress minmax problems because of the singularity of maximum stress, making it theoretically difficult to determine directly the sensitivity of the local objective functional in Eq. (9). Therefore, the Kreisselmeier-Steinhauser (KS) function is used to transform the local objective functional into the following smooth differentiable integral functional.

$$\max_{x \in \Omega} \frac{\sigma_M(\boldsymbol{x})}{\sigma_a} \quad \rightarrow \quad \frac{1}{\rho} ln \left\{ \frac{1}{\int_{\tilde{A}} dA} \int_{\tilde{A}} exp\left(\frac{\sigma_M(\boldsymbol{x})}{\sigma_a} \rho \right) dA \right\} \tag{13}$$

Where $\tilde{A} = A_1 + A_2$, A_1 and A_2 express the top and the bottom surface of shell, respectively. Moreover, when a constant ρ is sufficiently large, the maximum stress can be extracted.

5.3. Derivation of the shape gradient function

Letting $(\bar{\boldsymbol{u}}_0, \bar{w}, \bar{\boldsymbol{\theta}})$ and Λ denote the Lagrange multipliers for the state equation and volume constraints, respectively, the Lagrange functional L associated with this problem can be expressed as

$$L\left(\boldsymbol{u}_0, w, \boldsymbol{\theta}, \bar{\boldsymbol{u}}_0, \bar{w}, \bar{\boldsymbol{\theta}}, \Lambda\right) = \frac{1}{\rho} \ln \left\{ \frac{1}{\int_{\tilde{A}} dA} \int_{\tilde{A}} \exp\left(\frac{\sigma_M}{\sigma_a} \rho \right) dA \right\} + l\left(\bar{\boldsymbol{u}}_0, \bar{w}, \bar{\boldsymbol{\theta}}\right) - a\left(\left(\boldsymbol{u}_0, w, \boldsymbol{\theta}\right), \left(\bar{\boldsymbol{u}}_0, \bar{w}, \bar{\boldsymbol{\theta}}\right)\right) + \Lambda\left(M - M_0\right). \tag{14}$$

For the sake of simplicity, it is assumed that the sub-boundaries acted on by the non-zero external forces $\boldsymbol{N}$, $\boldsymbol{Q}$ and $\boldsymbol{M}$ do not vary (i.e., $\boldsymbol{V}$=0), that the forces acting on the shell surface $\boldsymbol{f}, \boldsymbol{m}, q$ do not vary with regard to the space and the iteration history s (i.e., $\dot{f} = \dot{m} = \dot{q} = 0$). The material derivative $\dot{L}$ of the Lagrange functional can be derived as shown in Eq. (15) below using the velocity field $\boldsymbol{V}$.

$$\dot{L} = \frac{\int_{\tilde{A}} exp\left(\frac{\sigma_M}{\sigma_a}\rho\right)\frac{\partial \sigma_M}{\partial \sigma_{\gamma\delta}}\sigma'_{\gamma\delta}dA}{\sigma_a \int_{\tilde{A}} exp\left(\frac{\sigma_M}{\sigma_a}\rho\right)dA} - a\left((\boldsymbol{u}'_0, w', \boldsymbol{\theta}'),(\bar{\boldsymbol{u}}_0, \bar{w}, \bar{\boldsymbol{\theta}})\right)$$

$$+ l\left(\bar{\boldsymbol{u}}'_0, \bar{w}', \bar{\boldsymbol{\theta}}'\right) - a\left((\boldsymbol{u}_0, w, \boldsymbol{\theta}),(\bar{\boldsymbol{u}}'_0, \bar{w}', \bar{\boldsymbol{\theta}}')\right) + \Lambda'(M - M_0) + \langle G\boldsymbol{n}, \boldsymbol{V}\rangle, \quad \boldsymbol{V} \in C_\Theta, \quad (15)$$

$$\langle G\boldsymbol{n}, \boldsymbol{V}\rangle \equiv \int_A G\boldsymbol{n}\cdot\boldsymbol{V}dA = \int_A G\boldsymbol{V}_n dA$$

$$G = -\{C_{\alpha\beta\gamma\delta}(u_{0\alpha,\beta} + \frac{h}{2}\theta_{\alpha,\beta})(\bar{u}_{0\gamma,\delta} + \frac{h}{2}\bar{\theta}_{\gamma,\delta}) - C_{\alpha\beta\gamma\delta}(u_{0\alpha,\beta} - \frac{h}{2}\theta_{\alpha,\beta})(\bar{u}_{0\gamma,\delta} - \frac{h}{2}\bar{\theta}_{\gamma,\delta})\} + hH\Lambda$$
$$+ \frac{H\, exp\left(\frac{\sigma_M}{\sigma_a}\rho\right)}{\int_{\tilde{A}} exp\left(\frac{\sigma_M}{\sigma_a}\rho\right)dA} - \frac{H}{\int_{\tilde{A}} dA} + Hf_\alpha \bar{u}_{0\alpha} - Hm_\alpha\bar{\theta}_\alpha + Hq\bar{w} \quad . \quad (16)$$

Where C_Θ is the suitably smooth function space that satisfies the constraints of domain variation. H denotes twice the mean curvature.

The optimality conditions of the Lagrangian function L with respect to $(\boldsymbol{u}_0, w, \boldsymbol{\theta})$, $(\bar{\boldsymbol{u}}_0, \bar{w}, \bar{\boldsymbol{\theta}})$ and Λ are expressed as shown below.

$$a((\boldsymbol{u}_0, w, \boldsymbol{\theta}),(\bar{\boldsymbol{u}}'_0, \bar{w}', \bar{\boldsymbol{\theta}}')) = l((\bar{\boldsymbol{u}}'_0, \bar{w}', \bar{\boldsymbol{\theta}}')), \quad (\boldsymbol{u}_0, w, \boldsymbol{\theta}) \in U, \quad \forall(\bar{\boldsymbol{u}}'_0, \bar{w}', \bar{\boldsymbol{\theta}}') \in U \ , \quad (17)$$

$$a((\boldsymbol{u}'_0, w', \boldsymbol{\theta}'),(\bar{\boldsymbol{u}}_0, \bar{w}, \bar{\boldsymbol{\theta}})) == \frac{\int_{\tilde{A}} \exp\left(\frac{\sigma_M}{\sigma_a}\rho\right)\frac{\partial \sigma_M}{\partial \sigma_{\gamma\delta}}\sigma'_{\gamma\delta}dA}{\sigma_a \int_{\tilde{A}} \exp\left(\frac{\sigma_M}{\sigma_a}\rho\right)dA}, \quad (\bar{\boldsymbol{u}}_0, \bar{w}, \bar{\boldsymbol{\theta}}) \in U, \quad \forall(\boldsymbol{u}'_0, w', \boldsymbol{\theta}') \in U, \quad (18)$$

$$\Lambda(M - \hat{M}) = 0, \quad \Lambda \geq 0, \quad M - \hat{M} \leq 0 .$$

(19)(20)(21)

When the optimality conditions with respect to the state variable $(\boldsymbol{u}_0, w, \boldsymbol{\theta})$, the adjoint variable $(\bar{\boldsymbol{u}}_0, \bar{w}, \bar{\boldsymbol{\theta}})$ and Λ are satisfied, Eq. (15) becomes

$$\dot{L} = \langle G\boldsymbol{n}, \boldsymbol{V}\rangle . \quad (22)$$

The shape gradient function $G\boldsymbol{n}$ (=$\boldsymbol{G}$) is applied to the free-form optimization method to determine the optimal design velocity field $\boldsymbol{V}$.

6. Free-form optimization method for shell structure

The free-form optimization method described here is initially proposed by Shomoda for the shape optimization problem for shells [1]. The method is based on the H^1 gradient method in a Hilbert space [9][10]. It is a node-based shape optimization method that can treat all nodes as design variables and does not require any design variable parameterization.

With this method the negative shape gradient function $-\boldsymbol{G}(\boldsymbol{X})$ is applied as a distributed force to a pseudo-elastic shell structure in the normal direction to the surface under a Robin boundary condition(distributed spring constant $\alpha > 0$), and shape design constraint conditions as shown in Fig. 3. The shape gradient function is not applied directly to the shape variation but rather is replaced by a force. This makes it possible both to reduce the objective functional and to maintain the smoothness, i.e., mesh regularity. The analysis for the shape variation $\boldsymbol{V}$ is called velocity analysis, and the obtained $\boldsymbol{V}$ is used to update the shape. The governing equation of the velocity analysis for $\boldsymbol{V} = \{\bar{V}_{01}, \bar{V}_{02}, \bar{V}_3\}$ is expressed as Eq. (23).

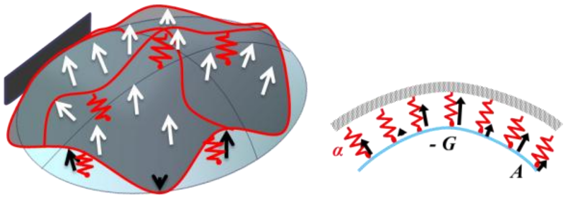

Fig. 3 Schematics of free-form optimization method for shell

$$a((\boldsymbol{V}_{0\beta}, V_3, \boldsymbol{\theta}), (\bar{\boldsymbol{u}}_0, \bar{w}, \bar{\boldsymbol{\theta}})) + \alpha \left\langle (\boldsymbol{V}\cdot\boldsymbol{n})\boldsymbol{n}, (\bar{\boldsymbol{u}}_0, \bar{w}, \bar{\boldsymbol{\theta}}) \right\rangle = -\left\langle G\boldsymbol{n}, (\bar{\boldsymbol{u}}_0, \bar{w}, \bar{\boldsymbol{\theta}}) \right\rangle, \quad (\boldsymbol{V}_{0\beta}, V_3, \boldsymbol{\theta}) \in C_\Theta, \quad \forall (\bar{\boldsymbol{u}}_0, \bar{w}, \bar{\boldsymbol{\theta}}) \in C_\Theta \ , \quad (23)$$

In problems where convexity is assured, this relationship definitely reduces the Lagrange functional in the process of updating the frame shape using the design velocity field $\boldsymbol{V}$ determined by Eq. (23)[1].

The optimal free-form frame structure is obtained by repeating the process consisting of (1) stiffness analysis, (2) adjoint analysis, (3) a sensitivity analysis for calculating the shape gradient functions, (4) velocity analysis and (5) shape updating. The analyses in the process (1), (2) and (4) are conducted using a standard general-purpose FEM code.

The advantages offered by this method are summarized as follows: (1) a smooth and natural surface can be obtained because the elastic tensor in the pseudo-elastic analysis serves as a mapping function and as a smoother for maintaining mesh smoothness, and its positive definitiveness is the necessary condition for minimizing the objective functional. (2) An optimal free-form surface is created because all the nodes can be moved as the design variable. (3) Mesh smoothing is simultaneously implemented in the shape changing process. (4) It can be easily implemented in combination with a commercial FEM code.

7. Calculated Results by the Free-form Optimization Method

In order to confirm its validity and practical utility for designing the optimal free-form of shell structures, the proposed method was applied to two design problems. As the Robin boundary condition in the velocity analysis, the earth spring constant was given as $\alpha = 20000$ in each design problem, which was equivalent to 1.2D (D: bending rigidity). Moreover, each FE model was discretized by constant strain triangular elements.

7.1. U-shaped bracket design problem

The first design example considered is a U-shaped bracket. The initial shape and the boundary condition of the stress analysis are illustrated in Fig. 4(a), in which nodal forces were applied in the inward direction of both edges. Fig. 4(b) shows the boundary condition of the velocity analysis, where all the edges were simply supported. The obtained optimal shape is shown in Fig. 5. Iteration convergence histories of the volume, the objective function (eqn. (13)) and the maximum value of von Mises stress are shown in Fig. 6. The values were normalized to those of the initial shape. Fig. 7(a) and (b) show the von Mises stress distribution of the initial shape and the optimized shape, respectively. It is clear that several beads were obtained along with the longitudinal direction of bending part, and the stress was reduced efficiently by the optimized shape. As shown in Fig. 6, the objective function was reduced by approximately 46%, and the maximum stress was reduced about 64% while satisfying the given volume constraint.

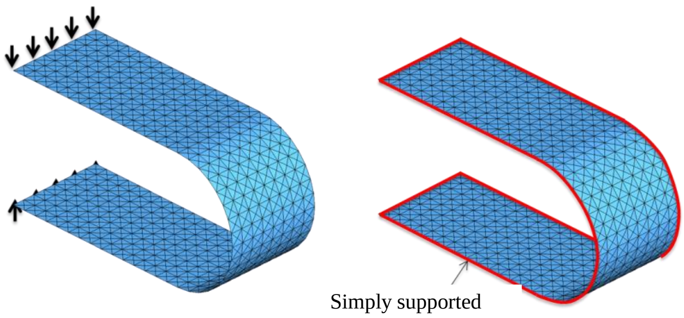

(a) Stress analysis (b) Velocity analysis

Fig. 4 Initial shape and boundary conditions of U-shaped bracket

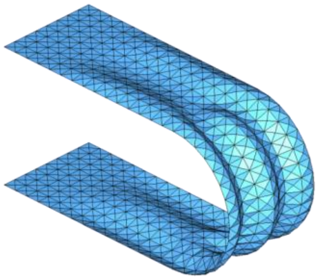

Fig. 5 Calculated result of U-shaped bracket

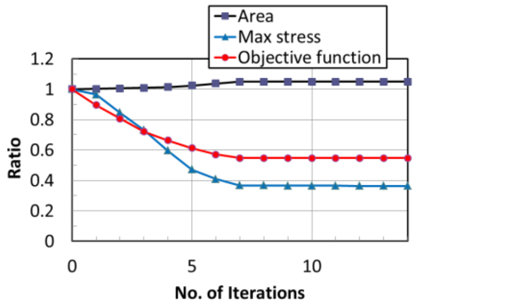

Fig. 6 Iteration histories of U-shaped bracket

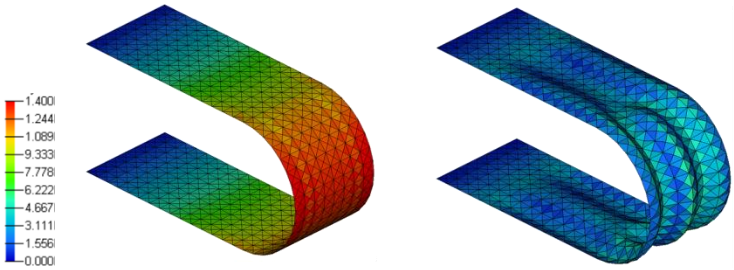

(a)Initial (b) Optimal

Fig. 7 Comparison of von Mises stress distribution of U-shaped bracket

7.2. Torsion arm design problem

A box-type shell structure with holes in the two flanks, as shown in Fig. 8, was optimized as an example of the practical structures. The initial shape is shown in Fig. 8(a) along with the boundary conditions of the stress analysis. In the stress analysis, the two through holes were clamped and downward distributed nodal forces were applied on the right side. The constraint conditions for the velocity analysis are shown in Fig. 8(b), where shapes of two flanks were assumed to do not vary. Moreover, the volume constraint was set at 1.05 times the initial value. As shown in Fig.9(a), the maximum stress occurs around the hole in the initial shape. The optimal shape obtained and the von Mises stress distribution is shown in Fig. 9(b). The shape variation in the upper and lower surfaces including the R parts of the box reduced the the maximum stress around the holes. The maximum stress was reduced by approximately 7% was reduced, and the practical utility of this method was verified.

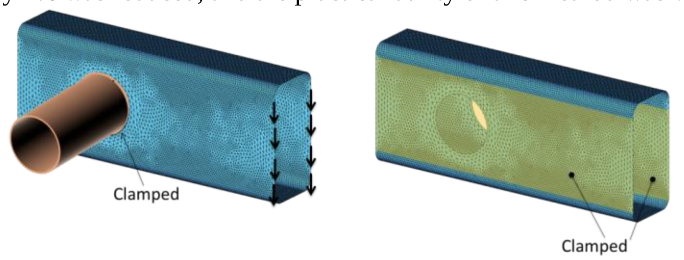

(a) Stress analysis (b) Velocity analysis

Fig. 8 Initial shape and boundary conditions of torsion arm problem

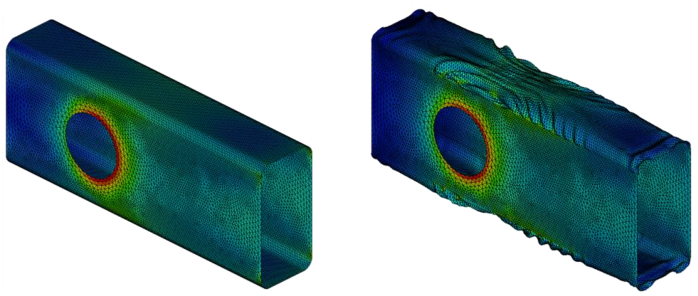

(a)Initial (b) Optimal

Fig. 9 Calculated result with von Mises stress distribution of torsion bar

8. Conclusions

This paper described the free-form optimization method for designing the optimal shapes of shell structures subject to a strength criterion. With the aim of minimizing the maximum von Mises stress under a volume constraint was formulated as a non-parametric shape optimization problem under the assumptions that the surface of shell is varied in the out-of-plane direction and the thickness is constant. In the proposed method, the issue of non-differentiability is avoided by transforming the local measure to an integral functional by using the *KS* function to transform the local objective functional into the smooth differentiable integral functional. The shape gradient function for this problem was theoretically derived and the method for the optimal design velocity using the adjoint variation was presented. As a result of analyzing the optimal shapes of two design problems, it was confirmed that the maximum von Mises stress was minimized and the optimal free-form shell with several beads was created, while maintaining the smoothness in each problem as expected.

9. References

[1] M. Shimoda, Free-Form Optimization Method for Designing Automotive Shell Structures, SAE, InternationalJournal of Passenger Cars- Electronic and Electrical Systems 4 (2011), pp. 42–54.

[2] Y. Liu, M. Shimoda, Multi-step Free-form Optimization of Shell Structures, Proceedings of 3rd International Conference on Engineering Optimization, EngOpt2012, Rio de Janeiro, Brazil, 1-5 July 2012.

[3] M. Shimoda, Y. Liu, M. Yonekura, Multi-objective Free-form Optimization of Shell Structures, Proceedings of 53rd Structures, Structural Dynamics, and Materials and Co-located Conferences, AIAA, Honolulu, Hawaii, 23 - 26 April 2012.

[4] M. Shimoda, Optimal free-form design of shell structures involving a natural frequency problem, Proceedingsof International Conference on Evolutionary and Deterministic methods for Design, Optimization and Control withApplications to Industrial and Social Problems, EUROGEN2011, Capua, Italy, September 2011. 3.

[5] E. Ramm, K. –U. Bletzinger and R. Reitiger, Shape optimization of shell structures, Int. J. Shell and Spatial Structures, 34 (2), pp. 103-121, 1993.

[6] T. Lindby and J. L. T. Santos, Shape Optimization of three-dimensional shell structures with the shape parameterization of a CAD system,Structural Optimization, 18, pp. 126-133, 1999.

[7] K. U. Bletzinger, M. Firl, et al., Optimal shapes of mechanically motivated surfaces, Comput. Methods Appl. Mech. Engrg., 199, pp. 324-333, 2010.

[8] Kreisselmeier, G. and Steinhauser, R., Systematic control design by optimizing a vector performance index, International Federation of Active Controls Syposium on Computer-Aided Design of Control Systems, (1979, Zurich).

[9] H. Azegami, A solution to domain optimization problems. Transactions of the Japan Society of MechanicalEngineers, Series A 60, 1479–1486 (1994)

[10] H. Azegami, S. Fukumoto, T. Aoyama, Shape optimization of continua using nurbs as basis functions. Struct. Multidisc. Optim. 47, 247–258 (2013)